Laboratory Experimentation of Stereo Vision-Based Relative Navigation with Unknown Spinning Spacecraft

Setareh Yazdkhasti, Steve Ulrich, and Jurek Z. Sasiadek
Department of Mechanical and Aerospace Engineering
Carleton University
Ottawa, Ontario, K1S 5B6, Canada
Email: setareh.yazdkhasti@carleton.ca

***Abstract*—In this paper, a vision-based relative navigation strategy applicable for an unknown and spinning target object in space is presented. Specifically, the relative navigation system uses a calibrated stereo monochrome camera, and is developed for estimating the relative position, linear velocity and angular velocity between the inspector spacecraft and the unknown target object, while minimizing the computational requirements. Experimental results in a dark room with a scaled model of a spacecraft spinning about its major axis of rotation are reported to demonstrate the performance and applicability of the navigation system for small inspection spacecraft.**

I. Introduction

Visual detection and tracking of a uncooperative, and possibly spinning space object is an important spacecraft robotics technology which enables various proximity operations, such as robotic capture, on-orbit servicing, inspection, and orbital debris removal. To achieve such challenging space robotic missions, the relative motion between the inspector and the target vehicle needs to be accurately determined such that the inspector spacecraft could perform proximity operation maneuvers in a safe and efficient way. Over the last decade, vision-based navigation systems have been extensively used to address the problem of relative motion determination, due to their low cost, mass, and power requirements, compared to active sensor-based techniques (e.g., laser range finder) [1] [2]. In particular, laboratory experimentations of cooperative vision-based navigation systems relying on known fiducial markers installed on the target vehicle were recently reported by Romano et al. [3] at the Naval Postgraduate School, and Tweddle and Saenz-Otero [4] at the Massachusetts Institute of Technology (MIT). Such cooperative vision systems were also extensively used actual on-orbit missions. For example, the Space Vision System (SVS) [5] monitored and tracked a pattern of special dots installed on the International Space Station. As the Space Station moved, the system tracked the changing position of the dots, and calculated the relative motion between the two vehicles. Similarly to SVS, Orbital Express' advanced video guidance sensor used photogrammetric algorithms to determine the six degree-of-freedom pose, i.e., the relative position and orientation between both spacecraft. Laser diodes were also used to illuminate retro reflective markers installed on the target spacecraft, to filter out other light frequencies, making it more immune to varying lighting conditions [6].

However, when the target spacecraft is uncooperative and has no known fiducial markers (LEDs, known visual patterns or dots), such vision systems cannot be used [7]. It is therefore required to develop a strategy that does not rely on such markers, i.e., a relative navigation system applicable for unknown, uncooperative, and possibly spinning, target spacecraft. Most of existing work in the literature that address the problem of uncooperative relative vision-based navigation assume the existence of a CAD model of the unknown object [8], [9]. For example, Neptec's TriDAR system [10] employs stereo camera and an on-board three-dimensional model, which uses a variant of the so-called iterative closest point (ICP) to match a three-dimensional model to the measurement points obtained from stereo matching. Jasiobedzki et al. [11] proposed a geometric probing approach that combines a voxel template set and a binary decision tree to prevent the ICP from reaching a local minimum. Tomasi and Takeo [12] developed a model-based solution in which factorization method uses multiple images taken by a monocular camera to measure the relative orientation between two spacecraft. As mentioned earlier, these methods are only suitable when prior knowledge of the geometry of the target spacecraft is available.

Recently, the MIT Space Systems Laboratory developed the Visual Estimation for Relative Tracking and Inspection of Generic Objects (VERTIGO) experimental facility to enable research and development of noncooperative vision-based relative navigation techniques that rely solely on optical stereo camera hardware and an on-board IMU. In 2013, on ISS Expedition 34, a relative navigation strategy to determine the relative position and linear velocity was validated with the SPHERES free-flyer nanosatellites maneuvering in a six degree-of-freedom microgravity environment, inside the ISS Japanese Experiment Module (JEM) [13]. Some shortcomings of this particular experiment were that: (1) the lightning conditions were not realistic (i.e., typical lighting conditions inside the ISS JEM), and (2) the target object was not covered with any highly-reflective and textured material inherent to any spacecraft, such as solar arrays and panels covered with

978-1-4799-8701-6/15/$31.00 ©2015 IEEE.

Multi-Layer Insulation (MLI) material. Additionally, textured stickers were placed on the target object to facilitate the image processing algorithms.

This work builds upon the VERTIGO experiment by validating a simple noncooperative vision-based relative navigation technique in a more realistic environment. Specifically, the proposed approach is tested in a dark room, with a directional light source pointed at the spinning target spacecraft model (1/50th scale model of RADARSAT-1) covered with highly reflective material. Similarly to VERTIGO, the proposed navigation system is based on image processing algorithms, which determine the relative position and velocity between both vehicles. Additionally, a simple way to calculate the angular velocity from the determined relative position is experimentally validated. This paper is organized as follows: Section II provides a description of the image processing strategy used to determine the relative position, velocity and angular velocity. Section III describes the testbed facility and reports laboratory experiments. Finally, conclusions are provided in Section IV.

II. Relative Navigation Approach

The proposed relative navigation approach calculates the relative position, velocity and angular velocity between a spinning target object and an inspector spacecraft equipped with a pair of calibrated stereo grayscale cameras. Calibration is required to remove any lens distortions adjust for any misalignment between the lenses, as well as between the two image sensors themselves. This was done by using the OpenCV library [14].

The first step is to capture raw stereo images from the stereo cameras. However, it is important to note that, when observing an object in motion such as a spinning spacecraft both stereo cameras must be accurately synchronized. Also, the exposure time must be set low enough to minimize motion blur effects. Second, a rectification is performed to overlap features of the stereo images in order to compare them through the epi-polar geometry.

The second step is to extract and match features points between the two cameras. A significant amount of research has been done in the development of different algorithms for feature detection and matching over the last decades [15]–[17]. Two of the more well-known techniques that are invariant to scale and rotation are the so-called Scale Invariant Feature Transform (SIFT) [18] and Speeded Up Robust Feature (SURF) [19]. The SURF [19] descriptor was chosen as it has proved to be highly efficient in terms of scale-invariance and rotation, while being highly robust against several deformations. Additionally, the SURF method has the ability for real-time applications as a result of using integral images and box filters. However, detecting and matching features with SURF often results in false matches (outliers) that must be rejected. To this end, a Random Sample and Consensus (RANSAC) algorithm [20] was herein used to reject outliers.

The third step is to compute a stereo disparity map. Due to its speed and simplicity, the Sum of Absolute Differences (SAD), was selected for this purpose. SAD is an algorithm that determines the similarity between a square window in the left image and another window in the right image, by calculating the absolute difference between each pixel in the left window and the corresponding pixel in the right window being used for comparison. These differences are summed to create a simple metric of block similarity. Specifically, given an image (in which each pixel (u,v) corresponds to a projection of a three-dimensional point onto camera focal plane) has a grayscale intensity value $I(u,v)$, an error function can be computed as

$$\Phi_{SAD}(u,v) = \sum_{x=-M_1}^{M_1} \sum_{y=-M_2}^{M_2} | I_L(u+x+d,u+y) - I_R(u+x,u+y) | \tag{1}$$

where $(2M_1+1)\times(2M_2+1)$ is the size of window, I_L is the intensity of a pixel in the left camera image, I_R is the intensity of corresponding pixel in right camera image, and d is the disparity, i.e., the position difference of a given pixel. This value must then be optimized by minimizing the SAD error function, such that the optimized disparity, denoted by $d^*(u,v)$ is given by

$$d^*(u,v) = \arg\ \min\ \Phi_{SAD}(u,v) \tag{2}$$

This block-matching algorithm is known to yield good performance, and the confidence estimate can be used to effectively mask out regions of high noise. Selection of block size is a trade-off between disparity map noise and accuracy. Once the disparity map is computed, the points are triangulated to compute a three-dimensional point cloud, as follows

$$Z_i = -\frac{T_x}{u} f - v \tag{3}$$

$$X_i = -C_x - u\frac{Z}{f} \tag{4}$$

$$Y_i = -v - C_y\frac{Z}{f} \tag{5}$$

where X_i, Y_i, and Z_i denote the three-dimensional Cartesian position of a given point i, with respect to a reference frame that has its origin at the center of the left camera focal plane and its z-axis being parallel to the optical axis of the cameras, f is the focal length of the left camera, and C_x and C_y are the principal point coordinates in pixels. The mean value of this point cloud is calculated and used as the estimate for the geometric center of the target object as follows

$$X = \sum_{i=0}^{N} X_i/N, \qquad Y = \sum_{i=0}^{N} Y_i/N, \qquad Z = \sum_{i=0}^{N} Z_i/N \tag{6}$$

The relative velocity is computed from the relative position using a first-order difference. An example of the result of implementing the stereo vision-based navigation strategy is shown in Fig. 1, where the left image shows the original image from the left camera, whereas the right-hand image shows the thresholded stereo disparity map. The green dot in the right image corresponds to the location of the geometric center, and

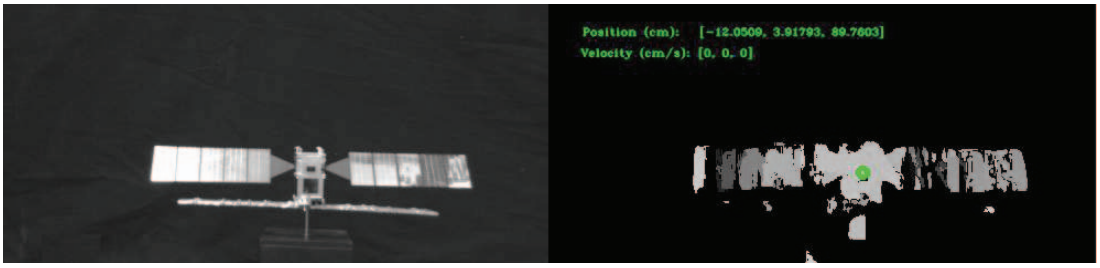

Fig. 1. Stereo disparity map.

the relative position and velocity of this particular point are shown as green text overlaid on the left-hand image.

Assuming that the target spacecraft is asymmetrical and rotates only about its major axis of inertia, the position along the Z component of the relative position vector will oscillate periodically back and forth following a sinusoidal form. This is a reasonable assumption since, by virtue of the *major-axis rule*, a spin about the major axis of inertia is the only stable rotational motion. Indeed, a major-axis spin represents a minimum of kinetic energy and thus most spacecraft can be expected to have a major-axis spin given sufficient time on orbit (due to energy dissipation). The angular velocity about the major axis of rotation can then be determined directly from the period of this cyclic variation in relative position measurements. Sequential snapshots of the spinning target spacecraft undergoing one revolution are provided in Fig. 2.

III. Experimental Results

In this section, the testbed that was developed to experimentally validate the proposed stereo vision-based relative navigation strategy is presented and then, results illustrating the performance of the approach in estimating both relative position and linear velocity, as well as angular rate between the inspector and the unknown spacecraft are reported.

A. Experimental Testbed

A laboratory testbed was developed to experimentally validate the vision-based technique described in this work. The testbed consists of a pair of calibrated and synchronized stereo monochrome uEye UI-1220LE USB cameras with a baseline of 80 mm observing a 1/50th scale motor of RADARSAT-1 Earth-observation spacecraft which is attached to the shaft of a DC motor, hence emulating a major-axis spin. The rotational speed of the high-gear ratio motor can be controlled between 1 and 10 RPM through an Arduino microcontroller. The two USB cameras are connected to a computer to compute, in real-time, the relative position and velocity of the rotating model. Because the model spacecraft does not have any fiducially markers, this setup is representative of a non-cooperative spinning target scenario. Moreover, unlike the VERTIGO experiment, the body of the spacecraft model is built from highly-reflective and specular wavy Multi-Layer Insulation (MLI) material, and with tinted mirrors that emulate solar panels, thereby rendering relative navigation process significantly challenging. A single light source simulating orbital directional lightning condition is also employed, with the result that optical features change drastically depending on orientation of the model spacecraft.

TABLE I
Camera characteristics

Characteristics	Description
Manufacturer	uEye
Model	UI-1220LE
Sensor	CMOS
Connection	USB 2.0
Shutter	Global
Optical class	1/3”
Focal length	2 cm
Maximum framerate	87.2 fps
Resolution	752 x 480
Pixel format	8 bit

B. Results

Using the technique described in the previous section, three-dimensional relative position and velocity components were determined, and the error results are provided in Figs.3 and 4, Figs.5 and 6, for a stationnary and a spinning target spacecraft, respectively. Note that these error signals were generated by comparing the outputs of the relative vision-based navigation system with ground truth data obtained with a tape measure. As shown in these figures, the maximum position and velocity determination errors along each axis are on the order of 0.005 m and 0.01 m/s, and 0.1 m and 0.04 m/s for the stationnary and spinning case, respectively. Another experiment was performed to assess the performance at varying distances along the line-of-sight axis. To this end, the relative position was determined at four arbitrarily distances: 0.47, 0.64, 0.88, and 1.16 m. As indicated in Figs 7 and 8, the relative position error slightly grows with increased distance. This is explained by the fact that when the target is further away from the camera, there are less traceable features can be used by the algorithm. Finally, Fig. 9 illustrates the angular velocity error about the major axis of rotation of the target spacecraft when it is spinning at 10.6 rotations per minute (RPM).

Finally, the computational time of the main algorithmic element of the proposed relative navigation system, i.e., (1) computing and thresholding the stereo disparity map, (2)

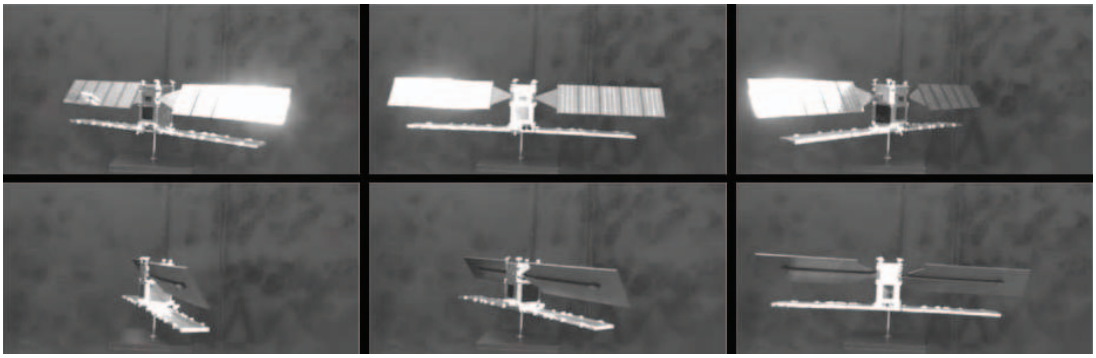

Fig. 2. Sequential pose of the spinning target spacecraft.

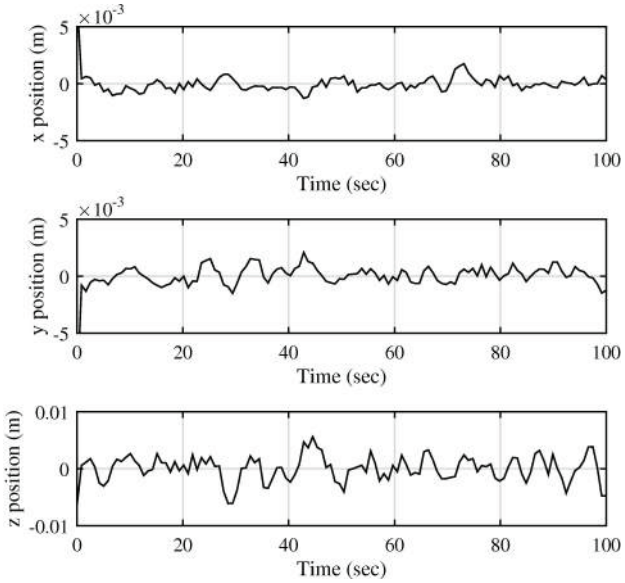

Fig. 3. Relative position errors for a stationnary target.

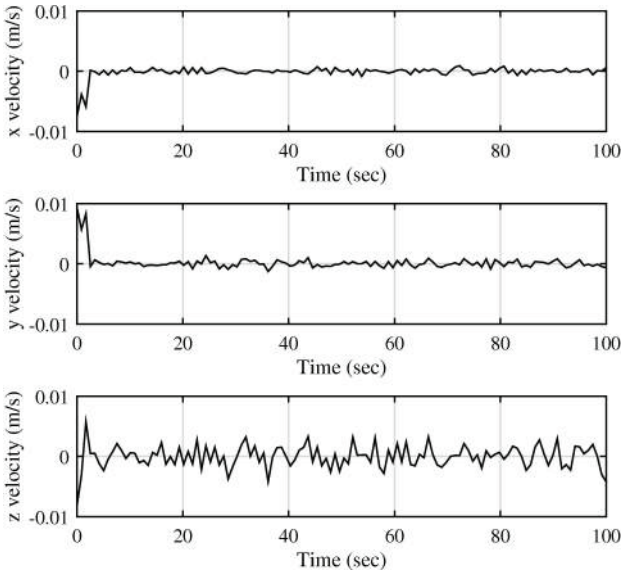

Fig. 4. Relative velocity errors for a stationnary target.

three-dimensional centroid, and (3) velocity calculation is reported in Table II. From this table, it is clear that the relative navigation system presented in this paper has a low computational footprint, where the majority of the computation time is spent in computing the disparity map from the stereo images.

TABLE II
COMPUTATIONAL REQUIREMENTS

Algorithm	Average Time (ms)
Compute disparity map	110.8
3D centroid	5.0
Position, velocity, and filtering	21.4

IV. CONCLUSIONS

In this paper, a simple strategy was proposed for determining the relative position, velocity, and angular velocity between

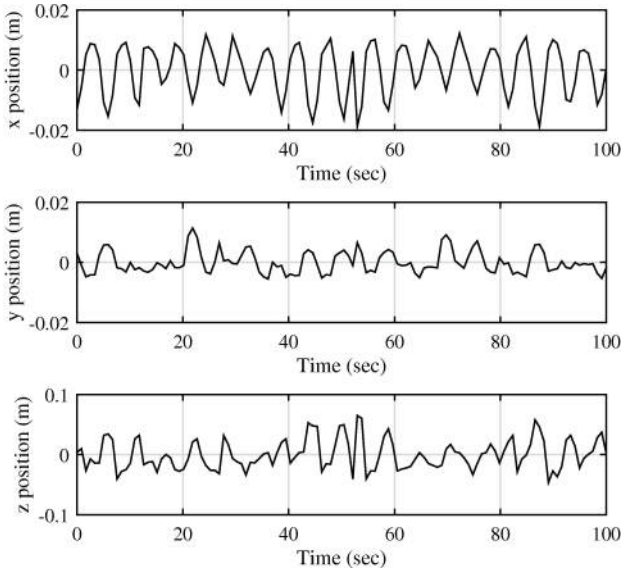

Fig. 5. Relative position errors for a spinning target.

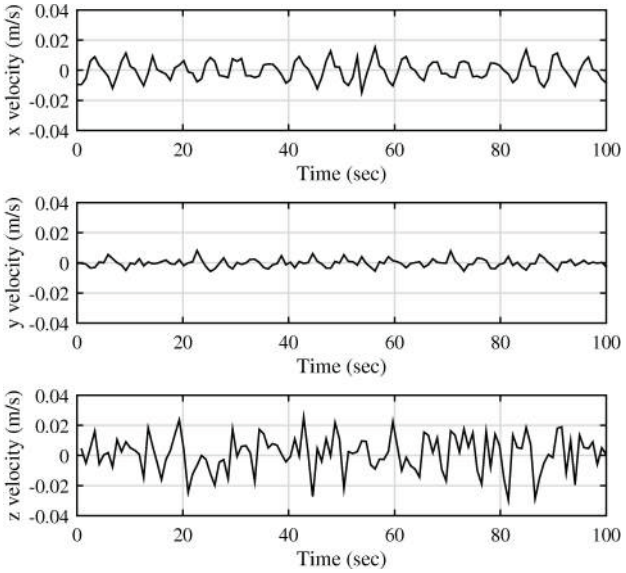

Fig. 6. Relative velocity errors for a spinning target.

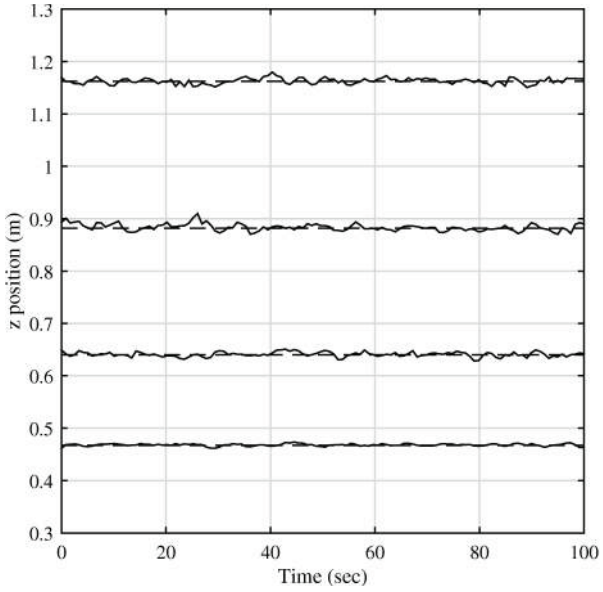

Fig. 7. Relative position at four different distances for a stationnary target.

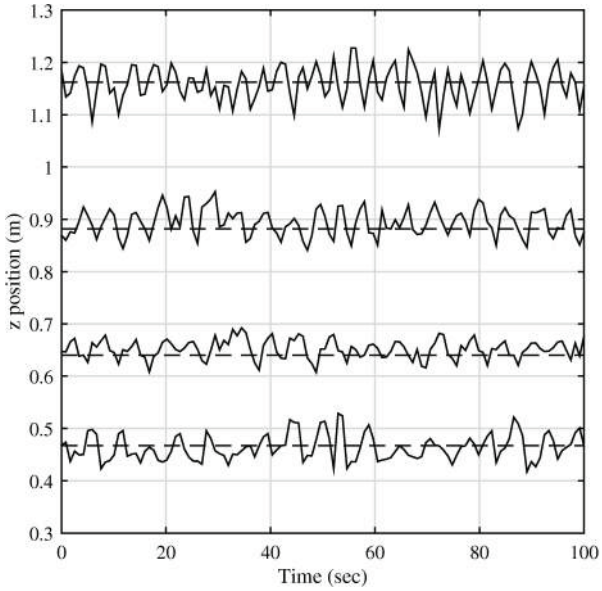

Fig. 8. Relative position at four different distances for a spinning target.

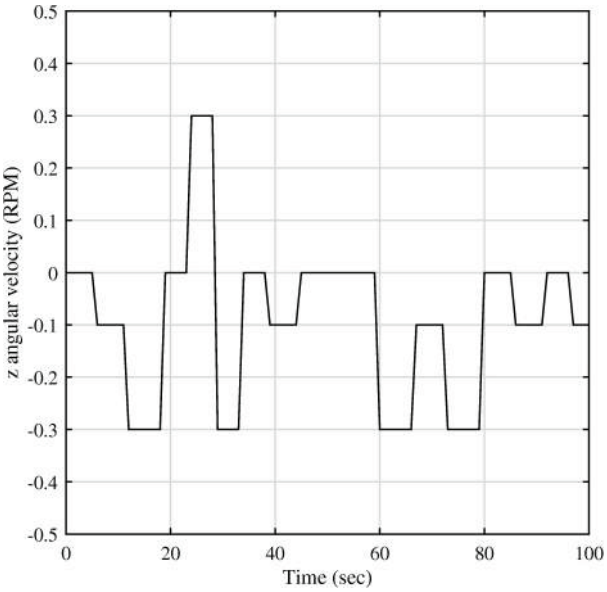

Fig. 9. Angular velocity error for a spinning target.

an inspector and an unknown spinning target spacecraft based only on calibrated stereo grayscale cameras. The proposed solution used the Speeded Up Robust Feature algorithm combined with the Random Sample and Consensus method to extract and match features points between the two cameras. Then, a three-dimensional stereo disparity was calculated from which the relative position and velocity were obtained. A simple way to determine the relative angular velocity was also presented. The relative navigation system was experimentally validated in a dark room environment with a scaled model of a satellite built with highly reflective material. Experimental results demonstrated that the simple noncooperative relative navigation system is applicable for real-time operations that require accurate performance. As future work, the development of a robust stochastic filter for obtaining the complete relative state vector (including the relative pose) with respect to an noncooperative spinning target will be investigated.

ACKNOWLEDGMENTS

The authors gratefully acknowledge the Canadian Space Agency for providing the CAD model of the RADARSAT-1 satellite from which the 1/50th scale model used in this work was built. The technical contributions from Jack Vedelago from Carleton University in the development of the testbed are also acknowledged.

REFERENCES

[1] Tarabini, L., Gil, J., Gandia, F., Molina, M. A., del Cura, J. M., and Ortega, G., "Ground Guided CX-OLEV Rendez-Vous with Uncooperative Geostationary Satellite." *Acta Astronautica*, Vol. 61, No. 1, 2007, pp.312-325.

[2] Lyn, C., Mooney, G., Bush, D., Jasiobedzki, P., King, D., Krishnasamy, R., Ng, H.-K., Ogilvie, A., Pennells, M., Pop, H., Rossi, S., and Umasuthan, M., "Computer Vision Systems for Robotic Servicing of the Hubble Space Telescope," *AIAA SPACE Conference & Exposition*, AIAA, Reston, VA, 2007; AIAA Paper 2007-6259.

[3] Romano, M., Friedman, D. A., and Shay, T. J., "Laboratory Experimentation of Autonomous Spacecraft Approach and Docking to a Collaborative Target," *Journal of Spacecraft and Rockets*, Vol. 44, No. 1, 2007, pp. 164-173.

[4] Tweddle, B. E., and Saenz-Otero, A., "Relative Computer Vision-Based Navigation for Small Inspection Spacecraft," *Journal of Guidance, Navigation, and Control*, doi: 10.2514/1.G000687.

[5] MacLean, S. G., and Pinkney, H. F. L., "Machine Vision in Space," *Canadian Aeronautics and Space Journal*, Vol. 29, No. 2, 1993, pp. 63-77.

[6] Howard, R., Heaton, A., Pinson, R., and Carrington, C., "Orbital Express Advanced Video Guidance Sensor," *IEEE Aerospace Conference*, Inst. of Electrical and Electronics Engineers, Piscataway, NJ, 2008, pp. 1-10.

[7] Flores-Abad, A, Ma, O., Pham, K., and Ulrich, S., "A Review of Space Robotics Technologies for On-Orbit Servicing," *Progress in Aerospace Sciences*, Vol. 68, 2014, pp. 1-26.

[8] Fuyuhito, T. , Kamimura, H., and Nishida, S., "Motion Estimation to a Failed Satellite on Orbit Using Stereo Vision and 3D Model Matching," *9th International Conference on Control, Automation, Robotics and Vision*, Inst. of Electrical and Electronics Engineers, Piscataway, NJ, 2006, pp. 1-8.

[9] Fuyuto, T., "Model Based Visual Relative Motion Estimation and Control of a Spacecraft Utilizing Computer Graphics," *21st International Symposium on Space Flight Dynamics*, Tolouse, France, 2009.

[10] Ruel, S., Luu, T., and Berube, A., "Space Shuttle Testing of the TriDAR 3D Rendezvous and Docking Sensor," *Journal of Field Robotics*, Vol. 29, No. 4, 2012, pp. 535553.

[11] Jasiobedzki, P., Greenspan, M., and Roth, G., "Pose Determination and Tracking for Autonomous Satellite Capture," *6th International Symposium on Artificial Intelligence and Robotics & Automation in Space*, St-Hubert, Canada, June 18-22, 2001.

[12] Tomasi, C., and Kanade, T., "Shape and Motion from Image Streams Under Orthography: A Factorization Method," *International Journal of Computer Vision*, Vol. 9, No. 2, 1992, pp. 137-154.

[13] Fourie, D., Tweddle, B. E., Ulrich, S., and Saenz-Otero, A., "Flight Results of Vision-Based Navigation for Autonomous Spacecraft Inspection of Unknown Objects," *Journal of Spacecraft and Rockets*, Vol. 51, No. 6, 2014, pp. 2016-2026.

[14] Bradski, G., and Kaehler, A., *Learning OpenCV: Computer Vision with the OpenCV Library*, O'Reilly, Cambridge, MA, 2008.

[15] Cyganek, B. and Siebert, J. P., *An Introduction to 3D Computer Vision Techniques and Algorithms*, Wiley, 2009.

[16] Rublee, E., Rabaud, V., Konolige, K., and Bradski, G., "ORB: An Efficient Alternative to SIFT or SURF," *IEEE International Conference on Computer Vision*, Inst. of Electrical and Electronics Engineers, Piscataway, NJ, 2011, pp. 2564-2571.

[17] Stockman, G., and Shapiro, L. G., *Computer Vision*, Prentice Hall, Upper Saddle River, NJ, 2001.

[18] Lowe, D. G., "Object Recognition from Local Scale-Invariant Features," *IEEE International Conference on Computer Vision*, Inst. of Electrical and Electronics Engineers, Piscataway, NJ, 1999, pp. 1150-1157.

[19] Bay, H., Ess, A., Tuytelaars, T., and Van Gool, L. "SURF: Speeded Up Robust Features", *Computer Vision and Image Understanding*, Vol. 110, No. 3, 2008, pp. 346-359.

[20] Fischler, M. A., and Bolles, R. C., "Random Sample Consensus: a Paradigm for Model Fitting with Applications to Image Analysis and Automated Cartography," *Communications of the Association of Computing Machinery*, Vol. 24, No. 6, 1981, pp. 381-395.